

STRUCTURAL INTEGRITY OF STEEL HYDROCARBON PIPELINES WITH LOCAL WALL DISTORTIONS

Aglaia E. Pournara

Dept. of Mechanical Engineering
University of Thessaly, Volos, Greece
email: agpournara@gmail.com

Spyros A. Karamanos

Dept. of Mechanical Engineering
University of Thessaly, Volos, Greece

Theocharis Papatheocharis

Dept. of Civil Engineering
University of Thessaly, Volos, Greece

Philip C. Perdikaris

Dept. of Civil Engineering
University of Thessaly, Volos, Greece

ABSTRACT

Local distortions on pipeline wall in the form of dents or buckles may constitute a threat for the structural integrity of the steel pipeline. In the present paper, experimental research supported by numerical simulation is reported to investigate the structural integrity of smoothly dented steel pipes. A series of six (6) full-scale experiments on 6-inch X52 pipes has been carried out, and numerical simulations have also been conducted. The dented steel pipes are subjected to cyclic loading (bending or pressure) in order to estimate their residual strength and remaining fatigue life. The finite element analysis simulates the experimental procedure for each type of deformation and loading case, in order to estimate the local stress and strain distributions at the dented region. Based on the numerical results, fatigue life is predicted and compared with the experimental results. The results of the present study are aimed at evaluating existing guidelines and methodologies towards appropriate assessment of local wall distortions in steel pipelines.

INTRODUCTION

Steel hydrocarbon pipelines may exhibit structural failure because of damage due to external interference, mechanical damage, or corrosion [1][2][3]. In the event of pipe wall dent, caused mainly by external interference, the pipeline may appear to fulfill its transportation function, provided that the steel material is adequately ductile and no cracks occur. However, the damaged area is associated with significant strain concentrations and, in the case of repeated loading cracks may develop, leading to fatigue failure. Therefore, the dented area and the associated strain concentrations may constitute a possible threat for the structural integrity of steel pipelines [3].

Evaluation of the remaining life of oil and gas transmission steel pipelines with local wall distortions has been considered a crucial issue for maintaining a reliable level of pipeline operation condition, and has triggered significant amount of research. Using four different two-dimensional shape functions to describe dent geometry, Ong [4] calculated local stresses at the pipe wall of a pressurized elastic pipe with a long smooth dent and found that the maximum local elastic stress varies between 14 and 21 times the value of the nominal hoop stress due to pressure. Ong et al. [5], using finite element simulation, calculated local elastic stresses at short and smooth dents, in pressurized dented cylinders. The peak elastic stress in short dents was found to be significantly less than in long dents. It was also concluded that the presence of local dents does not affect the burst capacity of the dented pipeline.

An experimental and numerical investigation of the fatigue resistance of offshore pipelines with plain (smooth) dents under cyclic pressure has been reported in [6]. A longitudinal wedge shaped denting tool was employed to dent 12 in. steel pipe specimens at depths ranging between 5% and 20% of their diameter. It was found that plain (smooth) dents with a depth larger than 5% may result in a reduction of the pipeline fatigue strength. Buitrago and Hsu [7], using a finite element simulation, investigated the fatigue response of non-pressurized tubular members containing relatively smooth dents and provided stress concentration factors in the form of parametric equations in terms of geometric parameters for axial and bending loads.

Recently, the effect of various defects (gouges, manufacturing or weld defects, corrosion) on the structural integrity of pipelines has been examined in a joint industry project [3][8][D], based on existing experimental and numerical

results. Considering a large number of publications regarding the ultimate capacity or the fatigue strength of defected or damaged pipelines, listed in [3][8], that study was aimed at the enhancement of the current methodologies and the identification of “gaps” in existing knowledge towards a “fitness-for-purpose” pipeline assessment. It was found that very limited data exist for the influence of buckles on the fatigue resistance of pipelines, while the fatigue capacity due to bending loads is not yet included.

Das et al. [9] conducted full-scale laboratory tests to investigate the post-wrinkling ultimate behavior of steel pipelines. The pipe specimens exhibited extreme ductile behavior and did not fail in fracture under monotonically increasing axisymmetric compressive axial loads and displacements. Fractures developed at the wrinkled region, however, when a wrinkled pipe specimen was subjected to cyclic strain reversals due to unloading and loading of primary loads. More recently, Dama et al. [10] presented experimental and numerical research conducted to assess the structural condition of buckled pipes, subjected to both bending and internal pressure. Fatigue failure under repeated loading and pipe burst have investigated, through three full-scale buckled pipe specimens and nonlinear finite element tools as shown in Figure 1. The maximum strain range from the finite element computations, and a simple S-N approach gave reasonable predictions for the number of cycles to failure observed in the tests. The results of that study demonstrate that under repeated loading, fatigue failure occurs in the buckled area at the location of maximum strain range.

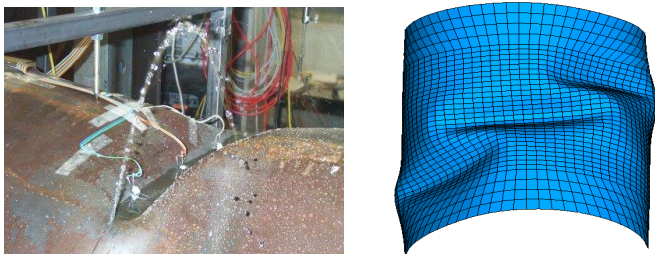


Figure 1: Fatigue cracking of buckled pipe under cyclic loading; test and numerical simulation [10]

The presence of dents has been recognized as a threat to pipeline integrity, mainly in terms of burst pressure capacity. Part 12 of API 579-1/ASME FFS-1 [11] code addresses the assessment of dents in pressurized components. In general, most of the available criteria employ a measurement of dent depth to determine its severity. International pipeline codes usually consider plain dents non-acceptable if they exceed a depth of 6% of the nominal pipe diameter. In a novel methodology proposed in Appendix R of the ASME B31.8 code [12], it is possible to estimate the maximum strain in a dent assuming the total strain in the dent as the combination of bending strain in the circumferential direction, the bending strain in the longitudinal direction and the membrane (stretching) strain in

the longitudinal direction. The value of this strain should be less than 6% for dent acceptability.

The present study is part of an extensive research program on the effects of local pipe wall distortions on the structural integrity of steel pipelines. Preliminary numerical work on the present research has been presented in [13]. In the present study, experimental research is presented supported by numerical simulation in order to investigate the residual structural integrity of dented steel pipes. A series of six (6) full-scale experiments on 6-inch pipes of steel grade X52 is carried out. The steel pipes are initially dented up to different depth values and, subsequently, they are subjected to further cyclic loading (bending or pressure) in order to estimate their residual strength and remaining life. Furthermore, finite element analysis is also conducted using appropriate material models to simulate the experimental procedure for each type of deformation and loading case, in order to calculate the stress and strain distributions at the dented region, so that fatigue life is calculated and compared with the experimental results. The results of the present study can be used for the assessment of local wall distortions in steel pipelines towards efficient pipeline integrity management.

SPECIMENS AND EXPERIMENTAL SET-UP

In this work, six (6) full-scale tests are performed, consisting of cyclic loading applied on dented pipes. First, the pipe specimens are dented with a wedge indenter at zero pressure, and subsequently, they are subjected to cyclic loading as follows:

- four (4) dented specimens are subjected to cyclic bending until fatigue cracking occurs in the low-cycle fatigue range,
- two (2) dented specimens are subjected to cyclic pressure loading for a significant number of cycles (5000 cycles) and then the pressure is raised monotonically until burst.

The six specimens are 1-meter-long X52 seamless 6-inch pipes with nominal thickness 4.78 mm ($\varnothing 168.3/4.78$), corresponding to $D/t = 35$. The specimen ends are capped with thick plates, to enable the application of internal pressure and the connection with adjacent pipe parts for the experimental set-up.

In the following paragraphs, the procedure of denting, cyclic bending and pressure loading are described. It is noted that denting and cyclic bending has been conducted at the laboratory facilities of the University of Thessaly, whereas the two pressure tests have been performed at the facilities of EBETAM S.A., located in Volos, Greece.



Figure 2: 6-inch X52 pipe specimens.

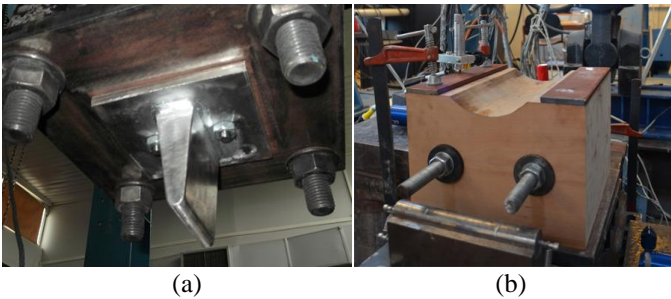


Figure 3: (a) Wedge denting tool and (b) wooden base to support pipe during bending.

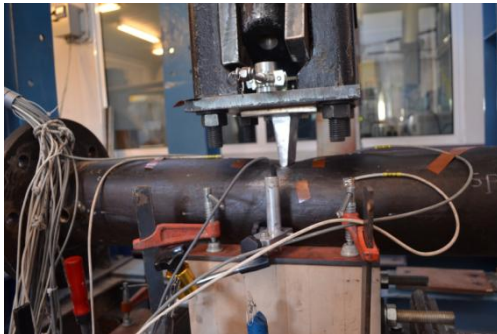


Figure 4: Denting set-up.



Figure 5: Instrumentation of pipe specimen.

Denting procedure

Denting is applied on the pipe specimens through the application of a rounded wedge indenter, shown in Figures Figure 3a and Figure 4, oriented perpendicular to the pipe axis, so that a smooth dent is formed on the pipe wall. The total wedge height is equal to 80 mm, the horizontal length is equal to 85 mm, and the radius of the rounded wedge is equal to 5 mm. As shown in Figure 3a, the wedge is bolted to the hydraulic actuator through the use of appropriate steel plates.

During denting, the specimen is supported on a wooden base (300×280×200) shown in Figure 3b. The top surface of the base was curved in order to prevent movement of the tubular specimen. Moreover, to avoid the development of strain and stress concentration in the pipe at the edge of the wooden base, the radius of base curve was chosen greater than the value of the nominal radius of the pipe. Furthermore, the wooden base was stiffened along both directions (length and height) with the use of steel rods in order to avoid excessive deformations of the wood material during the application of denting load.

Prior to denting, uniaxial strain gauges were installed on several critical points along the outside surface of the specimen, close to the region where the dent would be developed, in order to identify local strains during the denting procedure (Figure 5).

Cyclic bending set-up

The set-up employed for conducting cyclic bending on the dented specimens is shown in Figure 6 and Figure 7. The 1-meter long specimen is connected on either side to two heavy-walled 7-inch-diameter 650-mm-long tube segments ($\varnothing 193.7/10$) made of high-strength steel using a bolted connection (Figure 7). The entire system is 2.615-meters long, it is hinged at the two ends (Figure 8a) and it is connected to the 600-kN-force-capacity hydraulic actuator through a cross-beam and two wooden clamps (Figure 8b). This corresponds to a four-point bending structural system, where cyclic bending is applied through the vertical motion of the hydraulic actuator. The hinges of this 4-point bending set-up also minimizes the axial load introduced during the monotonic tests, because of the constraints applied by the wooden grips and the supports. Using appropriately located strain gauges the maximum value of this at maximum bending load axial force was calculated to be less than 8% of the cross-sectional axial yield strength and it is considered negligible.

Pressure test procedure

The two specimens have been pressurized with the use of a 400-bar-capacity water pump (Figure 9). Cyclic pressure has been applied with maximum and minimum values equal to 150 bar and 15 bar respectively, at a frequency of about 0.1 Hz. Following cyclic testing, the specimen was pressurized monotonically until burst.

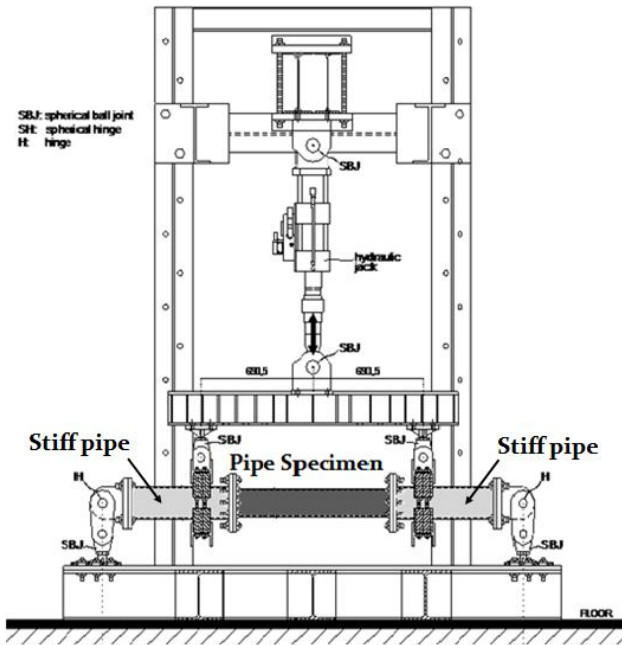


Figure 6: Configuration of the four-point bending experimental set-up.



Figure 7: Four-point bending experimental set-up.

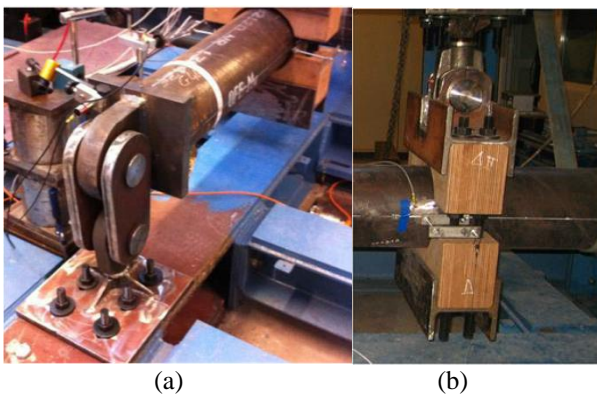


Figure 8: (a) bending specimen hinges and (b) wooden clamp.



Figure 9: Pressure application on specimens.

MATERIAL PROPERTIES AND WALL THICKNESS MEASUREMENTS

Material testing

Monotonic and low-cycle fatigue tests were performed on the X52 steel pipe material to determine material properties. Strip specimens have been extracted from the seamless 6-inch pipes, in the longitudinal direction and machined in accordance with the ASTM E606 standard. The material stress-strain curve was obtained from tensile coupon tests and is shown in Figure 10, indicating a yield stress (σ_Y) equal to 356 MPa, very close to the nominal value, and an ultimate stress (σ_{UTS}) equal to 554.7 MPa at about 18% uniform elongation.

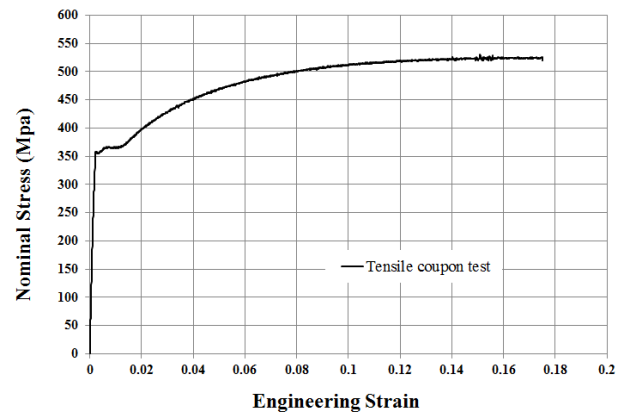


Figure 10: Material curve of X52 steel grade

In addition to tensile testing, a total of thirty (30) cyclic tests were performed on strip specimens with loading ratio R equal to -1 and 0. In those tests, the hysteresis loops at different strain ranges were determined and the fatigue ($\Delta\epsilon - N$) curve for the pipe X52 steel were developed. The tests have been performed in the facilities of FEUP in Porto[14] and the corresponding fatigue curve can be expressed by the following Coffin-Manson-Basquin equation.

$$\Delta\epsilon = 0.0102(2N)^{-0.1133} + 0.333(2N)^{-0.4807} \quad (1)$$

Thickness measurements

Prior to testing the specimens, thickness measurements were obtained using an ultrasonic device at specific points around several cross sections along the specimen's length (Figure 11). A mean thickness value was obtained equal to 5.026mm which is greater than the nominal value (4.78mm). Furthermore, the measurements did not show a significant variation of thickness with respect to this mean value. The value of 5.026mm will be used in all calculations in this paper.



Figure 11: Steel pipe specimens and thickness measurements via ultrasonic device.

EXPERIMENTAL RESULTS

Table 1, Table 2 and Table 3 show an overview of the experimental activity. Two values for the dent depth d have been considered, $d/D = 6\%$ and $d/D = 12\%$ (Table 1). The first value is equal to the dent acceptability limit used in practical applications, whereas the second value was chosen equal to twice this limit. During denting, the specimen was simply supported by the wooden base while its ends were totally unrestrained.

The first series of tests consists of cyclic bending tests on four (4) dented specimens (SP1d, SP3d, SP5d, SP6d) as shown in Table 2. The second part of the experimental work consists of pressure loading on two dented specimens (Table 3).

Denting results

The denting load is applied vertically through the hydraulic actuator at a very low speed until a maximum value of dent depth of about 16 (for SP1d, SP4d and SP6d) and 27 mm (for SP2d, SP3d and SP5d), and subsequently, the load was removed. The remaining dent depth after the elastic “spring back” is measured about 11mm and 21mm corresponding to $d/D = 6\%$ and $d/D = 12\%$ respectively. In Figure 12 the denting load-stroke curves for specimens SP5d and SP6d are presented. The increase of axial and hoop local strains is illustrated in Figure 13. The dent results are summarized in Table 1.

Table 1. Pipe denting results.

Specimens	residual depth d (mm)	normalized depth d/D (%)	Maximum force F_{max} (kN)
SP1d	10.245	6.08	69.26
SP2d	20.310	12.06	81.35
SP3d	20.198	12.00	83.29
SP4d	10.593	6.29	69.11
SP5d	20.263	12.04	81.75
SP6d	10.658	6.33	67.39

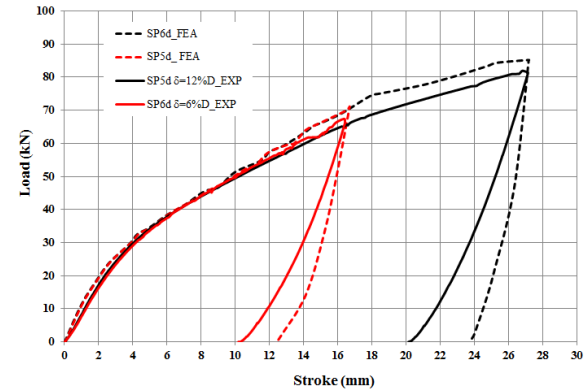


Figure 12: Load-stroke curves during denting procedure, for specimens SP5d and SP6d in comparison with the FEA results.

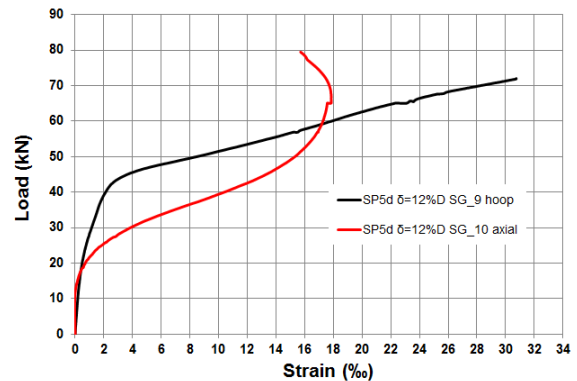


Figure 13: Longitudinal and hoop strain distribution during denting for specimen SP5d ($d/D = 12\%$).

Cyclic bending test results

After denting, the locally deformed pipe specimens are subjected to cyclic four-point bending using the set-up of Figure 6 and Figure 7, and a displacement-controlled pattern. The results are summarized in Table 2.

The loading sequence followed in dented specimens SP5d and SP6d is shown in Figure 14, in terms of the corresponding load-displacement curves. The two specimens were first bent beyond the limit load and subsequently, were subjected to cyclic loading at two stages. In all this procedure the dent was at the compression side of the specimen and the load ratio was equal to 0.1. Following a number of loading cycles of the bent specimen shown in Figure 15, each specimen failed because of fatigue crack at the dent “ridge”. The number of cycles to

failure is equal to 1,100 and 950 for specimens SP5d and SP6d respectively. The crack configuration for specimen SP5d is shown in Figure 16.

Specimens SP1d and SP3d are subjected to a different cyclic bending pattern, shown in Figure 17; both specimens are bent beyond the limit load [dent in compression]. Subsequently reverse bending is applied, so that the dented region is under tension, whereas the opposite region of the pipe exhibits compression. This loading situation results in local buckling at the opposite to the dent due to excessive compression. Under cyclic loading, fatigue cracks develop at the buckle “ridge”. The crack is quite similar to the one shown in Figure 16.

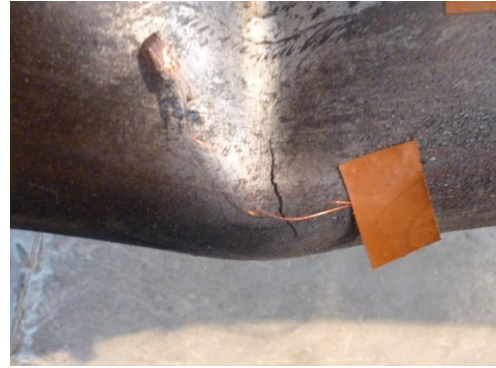


Figure 16: Pipe wall rupture of specimen SP5d due to cyclic bending loading at the dent “ridge”.

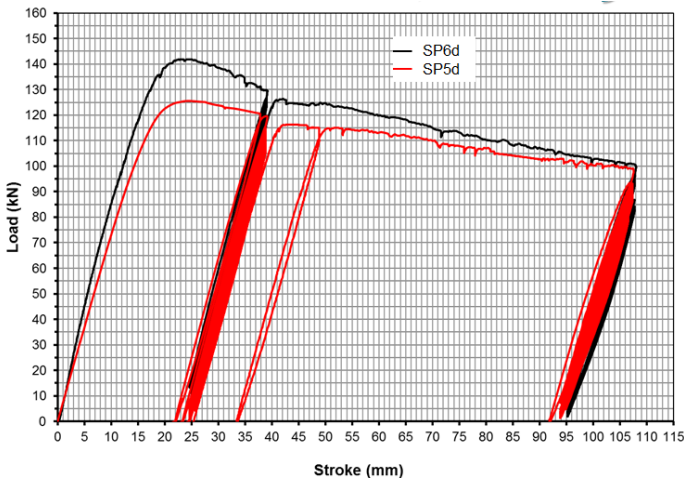


Figure 14: Load vs displacement curves for specimens SP5d and SP6d; monotonic and cyclic bending load.

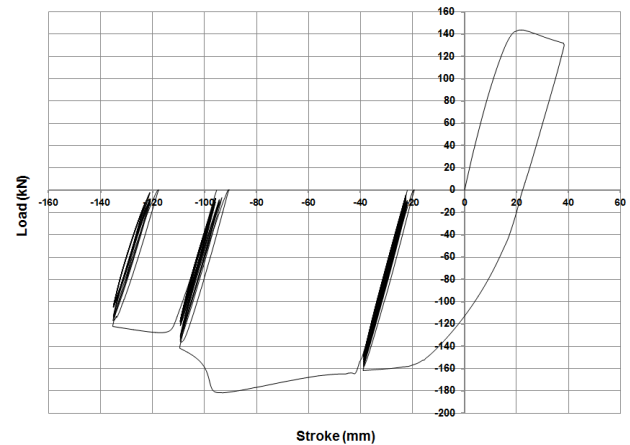


Figure 17: Load vs displacement curves for specimen SP1d; monotonic and cyclic bending load.



Figure 15: Dented specimen SP5d during cyclic 4-point bending.

Pressure tests results

Two dented specimens, namely SP2d and SP4d are tested under pressure loading. The results are summarized in Table 3. Both specimens are subjected to 5,000 cycles of pressure loading with minimum and maximum value equal to 1.5 MPa to 15 MPa respectively. No failure or damage has been detected due to cyclic loading. Subsequently, the specimens are subjected to monotonically increasing pressure until burst. Figure 18a. The pressure level at which rupture of pipe wall occurs is 32MPa and 31.6MPa for SP2d and SP4d respectively. It is interesting to notice that this value is quite close to the theoretical value of burst pressure estimated from the following simplified formula $\sigma_b = 2\sigma_{UTS} \frac{t}{D}$, where σ_{UTS} is the ultimate tensile stress. This result shows that the presence of a smooth dent on the pipe wall has no effect on the burst capacity of the pipe.

Furthermore, as shown in Figure 18a, in both cases the application of internal pressure resulted in a reduction of the dent size and a “smoothing” of the dented area. In addition, rupture of the pipe wall occurred away from the dent area, as

shown in Figure 18b, which was also observed in a similar test on a buckled pipe reported by Dama et al.[10].

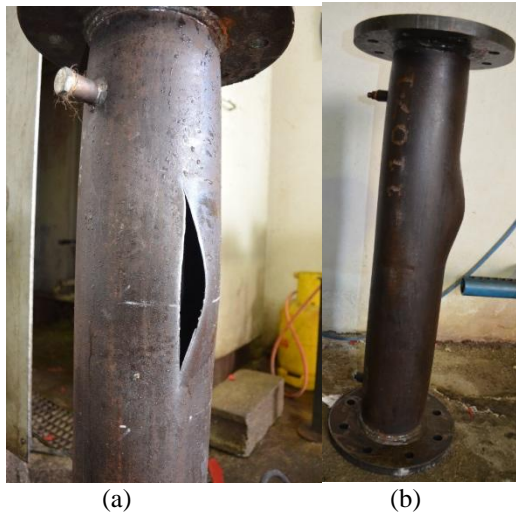


Figure 18:(a) Ruptured specimen due to increased internal pressure and (b) pipe wall rupture location (different than the dent location).

Table 2. Cyclic bending of dented specimens

Specimens	d/D (%)	Δu (mm)	N
SP5d	12.04	13.0	950
SP6d	6.33	13.0	1,100
SP1d*	6.08	16.0	1,400
SP3d*	12.00	16.0	1,200

*Dent in tension (reverse bending).

Table 3. Pressure loading of dented specimens

Specimens	d/D (%)	ΔP (MPa)	N	P_{burst} (MPa)
SP2d	12	13.5	5,000	32
SP4d	6	13.5	5,000	31.6

FINITE ELEMENT SIMULATION

Nonlinear finite element tools have been employed to simulate the development of the denting and the behavior of the dented pipes under cyclic bending and pressure loading. The simulations are conducted with finite element program ABAQUS 10.1., and the finite element models are capable of describing large displacements and strains, as well as inelastic effects rigorously. The pipe is simulated with four-node reduced-integration shell elements (S4R), which have shown to perform very well in nonlinear analysis problems involving large inelastic deformations of relatively thick-walled steel cylinders. A general view of the finite element model is shown in Figure 19.

In order to accomplish a good description of the dent profile, and the corresponding local stress and strain

distribution, the element mesh is rather dense at a two-diameter-long region, about the middle section of the pipe, where maximum deformation due to dent is located.

The finite element model consists of five parts; the denting tool, the pipe specimen, the wooden base that supports the pipe movement during indentation, and the two stiff pipe segments (see Figure 6) on either side of the specimen. The stiff pipe segments are simulated with beam elements of appropriate cross-sectional and material properties, with simply-supported conditions at the two ends. The thick end plates were modeled through a “kinematic coupling” constraint at the end nodes. Loading is applied at two points of those beam elements, corresponding to the locations of wooden grips.

To describe inelastic material behavior of the pipe specimens, a J_2 (von Mises) flow plasticity model with isotropic hardening is employed. The plasticity model is calibrated through appropriate uniaxial tensile tests on steel coupon specimens, extracted from the X52 6-inch pipes (yield stress equal to 356 MPa and ultimate stress equal to 554.7 MPa).

Simulation of pipe denting

The wedge-type denting tool is oriented in a direction perpendicular to the pipe axis, shown Figure 19. For reducing computational time, only the curved part of the wedge tool, which is in contact with the pipe, is modeled. The radius of the rounded wedge is equal to 5 mm identical to the one used in the experiments. The denting tool is designed as a non-deformable “analytical rigid” part. Contact interaction is imposed between the wedge surface and the outer surface of pipe wall.

The geometry of the wooden base, shown in Figure 19, is similar to the one used in real testing (Figure 3b) with dimensions 300mm×300mm and the upper surface properly curved in order to support the pipe model. Contact conditions are imposed between its surface and the pipe outer surface, which prevent penetration, but allow pipe uplifting.

The shape of the deformed model is shown in Figure 20. The pipe model rests on the support plate. During denting, the two pipe ends are non-restrained, resulting in a small uplifting of the pipe specimen. Following the experimental procedure, two values for dent depth are considered in this numerical study, namely 6% and 12% of the pipe diameter. Those are the values of the residual dent size after removal of the denting tool and the corresponding elastic rebound. The dent profile and the von Mises stress distribution around the dent region after elastic rebounding are shown in Figure 20. Moreover, force versus denting displacement curves are compared well with the experimental curves for both cases during the denting and after the wedge indenter removal, as shown in Figure 12.

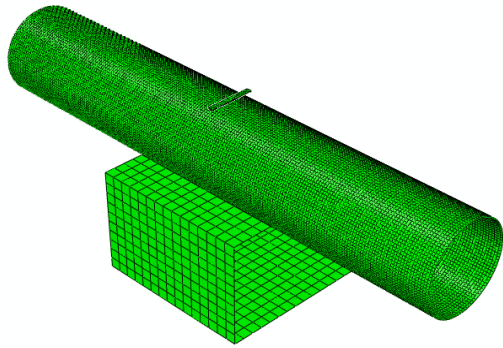


Figure 19: General view of the finite element model.

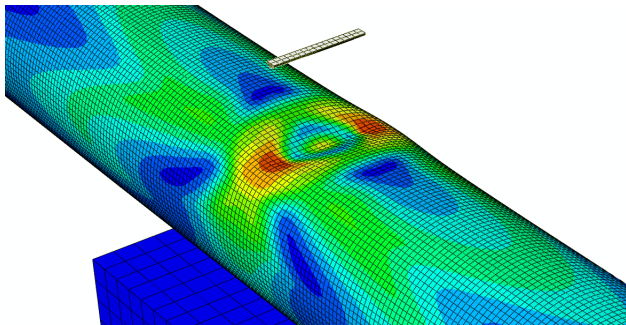


Figure 20: Finite element results for the dented specimen; distribution of von Mises stress at the outer surface of the pipe.

Cyclic bending of dented pipes

Following denting, cyclic bending loading of the dented pipe is simulated, similar to the experimental procedure. Figure 21 and Figure 22 show the load-displacement curves for those analyses, and compared fairly well with the experimental curves shown in Figure 14 and Figure 15. During the numerical simulation, cyclic bending loading of the specimens is performed at the loading stages corresponding to the experimental procedure. At each of these stages, a total of 10 cycles is performed numerically, and the corresponding range of maximum local strains in the longitudinal direction with respect to the pipe axis is measured and depicted in Table 4.

The deformed shape of specimen SP5d is shown in Figure 23, whereas in Figure 24 the shape of specimen SP3d (subjected to reverse loading) is depicted. In the latter shape, one may observe the dented area at the top of the specimen, which is under tension, and the buckled area, developed due to reverse bending at the opposite side of the pipe wall due to excessive compression. The buckled area is the one that corresponds to the maximum local strain range and where the fatigue crack develops.

Based on the values of local strain range, it is possible to employ the fatigue curve of the pipe material, expressed by equation (1), and apply Miner's rule to obtain a damage factor D_f , as follows:

$$D_f = \sum_i \frac{n_i}{N_i} \quad (2)$$

where N_i is the number of cycles corresponding to $\Delta\varepsilon_i$ obtained from the fatigue curve ($\Delta\varepsilon - N$) and n_i is the number of real cycles applied. Strains are measured at the outside surface. The results of this analysis are depicted in Table 4 for the four specimens under consideration. The values of the damage factor are quite close to 1, indicating a good correlation between test results and numerical analysis.

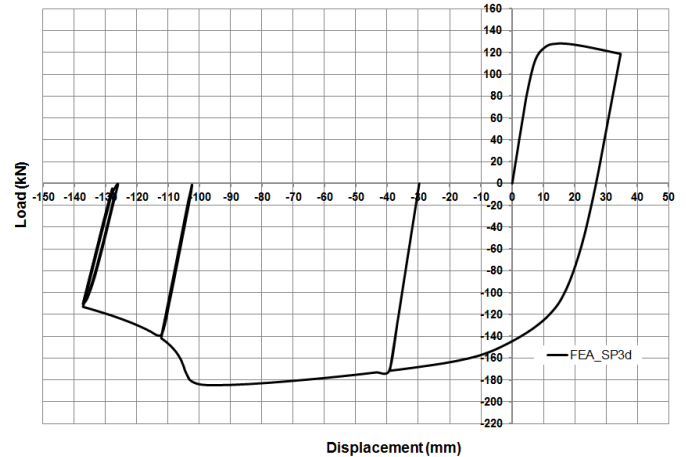


Figure 21: Load-displacement curve during bending of specimen SP3d (reverse and cyclic bending) obtained from finite element analysis.

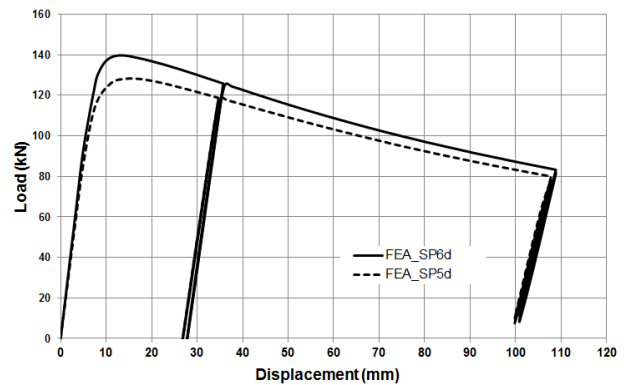


Figure 22: Load-displacement curve during bending of specimens SP5d and SP6d (monotonic and cyclic bending) obtained from finite element analysis.

Table 4. Fatigue analysis under cyclic bending

Specimen	Cycles applied N_i	$\Delta\varepsilon_{\max}$ (%)	D_f	$SNCF$
SP1d	500	0.306	1.13	1.239
	500	0.246		1.209
	400	1.914		11.98
SP3d	500	0.300	0.79	1.214
	500	0.248		1.219
	200	2.180		13.64
SP5d	500	0.790	1.11	4.184
	450	1.750		17.21
SP6d	500	0.603	1.15	3.193
	600	1.637		16.10

The value $\Delta\varepsilon_{\max}$ is the maximum local strain range in the axial direction at the dented (or buckled for SP1d and SP3d) (critical) region, and $\Delta\varepsilon_{nom}$ is the nominal strain range due to the applied loading, calculated through elementary mechanics of materials, considering the initial (intact) geometry of the tubular member. For the loading conditions under consideration, the strain concentration factor is computed through the measurement of the maximum strain variation in the longitudinal direction of the pipe, shown in Table 4. In the case of four-point bending, $\Delta\varepsilon_{nom}$ is calculated as follows:

$$\Delta\varepsilon_{nom} = \frac{2\alpha\Delta F}{E\pi D^2 t} \quad (4)$$

where ΔF is the range of total transverse load applied on the specimen, and α is the distance between the hinge support and the point of load application.

The values of strain concentration factor are shown in Table 4. The numerical results indicate that in the last stage of the bending curve, corresponding to severe deformation of the pipe, the $SNCF$ can obtain significant values. This is attributed to the fact that in that area, the pipe wall is quite distorted, and the cyclic loading is associated with severe folding/unfolding of the pipe wall. The calculated values of $SNCF$ are consistent with those reported by Dama et al [10] for locally buckled pipes.

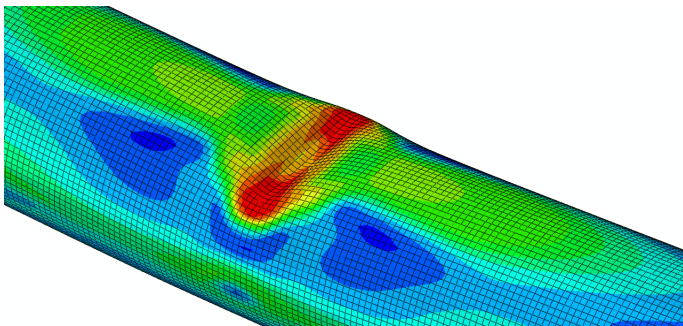


Figure 23: Deformed shape of specimen SP5d under cyclic bending conditions obtained from finite element analysis.

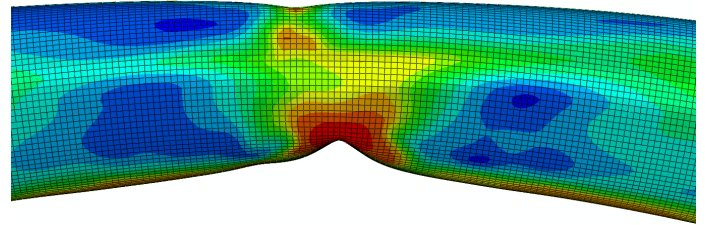


Figure 24: Deformed shape of specimen SP3d under cyclic bending conditions obtained from finite element analysis.

Simulation of pressure loading

Internal pressure is applied in the numerical model of the dented specimen. The results show that with increasing pressure, the dented profile “smoothens” (Figure 25), the dent size is decreased, and there is a tendency of gradual dent flattening, an observation also reported in [10]. Furthermore, for the range of cyclic pressure applied during the tests ($\Delta p=13.5$ MPa, with a maximum value of 15 MPa), the corresponding strain concentration factor $SNCF$ is small [A18]. This can verify the fact that the dented pipe is capable of sustaining 5,000 pressure cycles without failure or other damage, as observed experimentally.

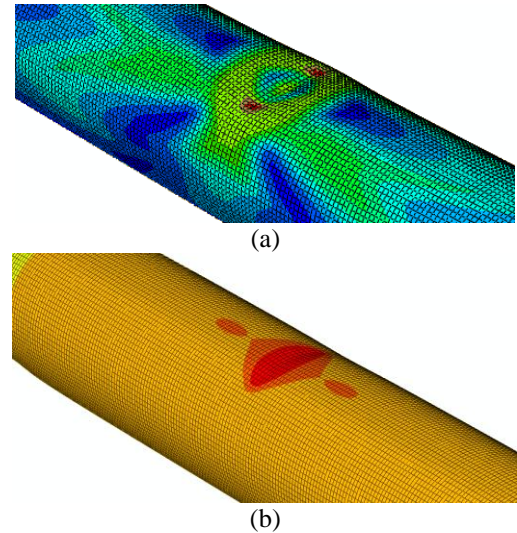


Figure 25: Dent geometry: (a) before pressure application for $d/D = 6\%$; (b) after pressure application.

The diagrams in Figure 26 present the response of the dented pipe upon monotonically increasing internal pressure. The increase of internal pressure results in decrease of dent depth and the dent profile tends to flatten. The maximum internal pressure obtained from the finite element analysis is equal to about $P_{\max} = 33$ MPa until convergence of solution is not possible due to excessive plastification of pipe wall. This pressure load is well compared with the burst pressure measured in the experiments.

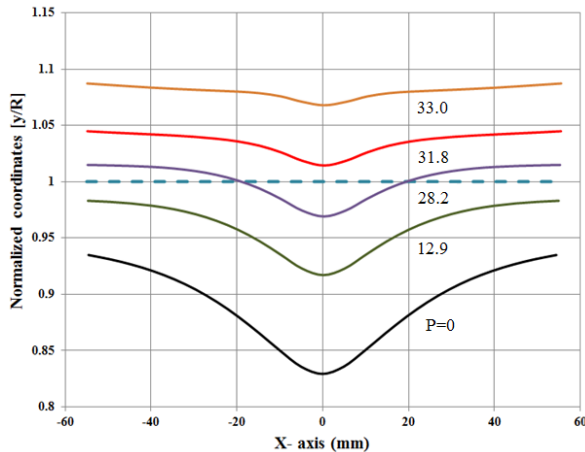


Figure 26: “Smoothing” of the dent profile with the increase of internal pressure

The coordinates in the vertical axis of Figure 26 refer to the position of the top outer wall generator for various pressure levels. The coordinates are normalized by pipe radius R.

CONCLUSIONS

Combining experimental testing and numerical simulation, the mechanical behavior of dented pipes under pressure and bending loading is examined. The experimental investigation consists of six (6) 6-inch-diameter X52-steel pipe specimens, initially dented at dent sizes of 6% and 12% which is twice as the maximum acceptable dent depth according to ASME B31.8 provisions ($d/D=6\%$). Subsequently, the specimens are tested under various loading conditions (bending and pressure). It is found that cyclic bending on four (4) dented specimens, causes fatigue cracking, located at the ridge of the deformed area, at about 1,000 loading cycles. In addition, an accurate finite element simulation of the experimental procedure (both denting and cyclic loading), together with the use of an appropriate fatigue curve for the pipe material, is considered as a sufficient tool for the prediction of pipeline fatigue life. The results indicated that the dented pipes with even a dent equal to 12% D can sustain a significant number of pressure cycles while the level of pressure and the location of the rupture are not affected by their presence. It is concluded that the fatigue life and the burst capacity of pipes with local dents, even larger than the maximum acceptable limit, have been severely underestimated by the current provisions.

ACKNOWLEDGMENTS

This research has been co-financed by the European Union (European Social Fund – ESF) and Greek national funds through the Operational Program "Education and Lifelong Learning" of the National Strategic Reference Framework (NSRF) - Research Funding Program: Heracleitus II. Investing in knowledge society through the European Social Fund. The authors would like to thank EBETAM A.E. for providing the facilities for pressure testing, as well as Dr. Abilio M. P. de Jesus from FEUP for providing the material test data.

REFERENCES

- [1] Doglione, R., and Firrao, D., 1998, “Structural Collapse Calculations of Old Pipelines,” *Int. J. Fatigue*, **20** (2), pp. 161–168.
- [2] Netto, T. A., Ferraz, U. S., and Estefen, S. F., 2005, “The Effect of Corrosion Defects on the Burst Pressure of Pipelines,” *J. Constr. Steel Res.*, **61** (8), pp. 1185–1204.
- [3] Cosham, A., and Hopkins, P., 2004, “The Effect of Dents in Pipelines—Guidance in the Pipeline Defect Assessment Manual,” *Int. J. Pressure Vessels Piping*, **81**, pp. 127–139.
- [4] Ong, L. S. 1991, “Derivation of Stress Associated with a Long Axial Dent in a Pressurized Cylinder,” *Int. J. Mech. Sci.*, **33** (2), pp. 115–123.
- [5] Ong, L. S., Soh, A. K., and On, J. L., 1992, “Experimental and Finite Element Investigation of a Local Dent on a Pressurized Pipe,” *J. Strain Analysis*, **27** (3), pp. 177–185.
- [6] Fowler, J. R., 1993, “Criteria for Dent Acceptability in Offshore Pipelines,” *Offshore Technology Conference*, OTC 7311, Houston, pp. 481–493.
- [7] Buitrago, J., and Hsu, T. M., 1996, “Stress Concentration Factors for Dented Tubular Members,” *Offshore Mechanics & Artic Engrg Conference*, OMAE, Vol. I, pp. 291–296.
- [8] Macdonald, K. A., and Cosham, A., 2005, “Best Practice for the Assessment of Defects in Pipelines—Gouges and Dents,” *Eng. Failure Anal.*, **12** (5), pp. 720–745.
- [9] Das, S., Cheng, J. J. R., Murray, D. W., 2007, “Prediction of the fracture life of a wrinkled steel pipe subject to low cycle fatigue load”, *Canadian Journal of Civil Engineering*, **34** (9), pp. 1131–1139.
- [10] Dama, E., Karamanos, S. A. and Gresnigt, A. M., 2007, “Failure of Locally Buckled Pipelines,” *ASME Journal of Pressure Vessel Technology*, **129**, pp. 272–279.
- [11] API 579/ASME FFS-1, “Fitness-for-Service,” 2007
- [12] ASME B31.8, 2007, Gas transmission and distribution piping systems. 2007 ed. ASME.
- [13] Pournara, A. E. and Karamanos, S. A., 2012, “Structural integrity of steel hydrocarbon pipelines with local wall distortions”, *Pressure Vessel and Piping Conference*, ASME, PVP2012-78131, Toronto, Canada
- [14] Fernandes A.A. et al., “Ultra Low Cycle Fatigue of steel under high-strain loading conditions,” 3rd Annual Progress Report of ULCF-RFCS Project, Porto, 2013

